NASA/TM—1998-208825

ARL–TR–1447

Model–Based Fault Diagnosis for Turboshaft Engines

Michael D. Green and Ahmet Duyar
Florida Atlantic University, Boca Raton, Florida

Jonathan S. Litt
Lewis Research Center, Cleveland, Ohio

National Aeronautics and
Space Administration

Lewis Research Center

November 1998

Acknowledgments

MODEL-BASED FAULT DIAGNOSIS FOR TURBOSHAFT ENGINES

Michael D. Green[1], **Ahmet Duyar**[1], and **Jonathan S. Litt**[2]

[1]*Department of Mechanical Engineering*
Florida Atlantic University, Boca Raton, FL 33431

[2]*Vehicle Technology Center*
U.S. Army Research Laboratory
Lewis Research Center, Cleveland, Ohio 44135

Abstract: Tests are described which, when used to augment the existing periodic maintenance and pre-flight checks of T700 engines, can greatly improve the chances of uncovering a problem compared to the current practice. These test signals can be used to expose and differentiate between faults in various components by comparing the responses of particular engine variables to the expected. The responses can be processed on-line in a variety of ways which have been shown to reveal and identify faults. The combination of specific test signals and on-line processing methods provides an *ad hoc* approach to the isolation of faults which might not otherwise be detected during pre-flight checkout.

Keywords: Fault detection, Fault diagnosis, Engine, Helicopter, Diagnostic tests

1. INTRODUCTION

This report presents the research work on the design of a model-based fault detection and diagnosis (FDD) system for use in turboshaft engine maintenance. The FDD system detects component malfunctions (faults) by monitoring engine output during maintenance testing. This work focuses on components related to fuel control actuation to demonstrate the applicability of the method. A previous study (Litt, *et al.*, 1995) presented a related scheme for detection of sensor faults.

Current engine maintenance procedures at the Aviation Unit Maintenance (AVUM) and Aviation Intermediate Maintenance (AVIM) levels are described in T700 (1981). There are several on-line and pre-flight checks which are performed currently on T700 engines (figure 1) in Blackhawk and Apache helicopters. These include the Health Indicator Test (HIT) check which is performed at flight idle and compares exhaust temperature to power level to make sure it is within range. On-line cockpit instrumentation indicates engine chips (metallic particles in the oil) and oil temperature and pressure limits. These provide information about the existence of a problem without determining the cause. An artificial intelligence-based diagnostic system (*Aerospace Engineering*, 1995) has been tried in order to get more information about individual components, but it only gives an indication of the likely source of the problem, if one is detected, and this often requires several steps after the testing is completed.

On the other hand, model-based fault detection methods compare the system's output to that of a model running simultaneously. Any difference beyond a threshold value signifies that a fault has occurred. The present work evaluates the faults using the approach developed and implemented by Litt, *et al.* (1995) and by Duyar, *et al.* (1994). The experimental modeling technique developed by Duyar, *et al.* (1995) is used to obtain the state space diagnostic model, i.e., the model used to determine faults. Test input signals for diagnosis purposes to be applied during maintenance of the engine have been explored and the most suitable chosen.

The model of the normal process developed by Duyar, *et al.* (1995) did not include the dynamics of fuel control actuation (the hydromechanical unit, HMU). The HMU output fuel flow rate was used as input to the model rather than the command signals from the electrical control unit (ECU) and the collective (figure 2). In the work reported here, the ECU and collective
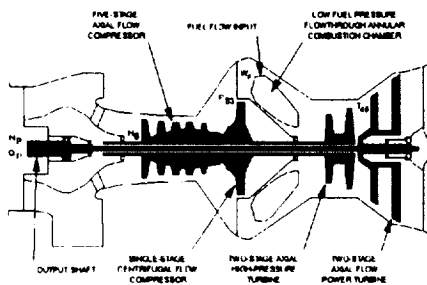
Figure 1 Cross section of a T700 turboshaft engine

Figure 2. T700 Macroscopic Open Loop Block Diagrams
(HMU is represented by simplified model)

command signals were used as inputs to an open-loop block diagram of a T700 turboshaft helicopter engine, which implicitly incorporates the HMU dynamics, thus converting the HMU's fuel flow to an output (figure 2). Further, in the present work the block diagram was derived such that the engine is separated from the rotor system. This strategy makes it possible for the resulting open-loop model to be used not only for FDD, but also for control design and system simulation when linked with an appropriate rotor system model.

The trouble-shooting procedures of Litt, et al., (1995) were studied together with information on the components involved found in Ballin (1988) and the T700 Training Manual (Prescott and Morris, 1987) to identify potential faults to be considered. Two potential actuator faults listed were selected to illustrate the method: an increase in friction in the torque motor and a clogging fuel metering valve. Two additional faults, which are outside the actuation system, were also modeled: degradation of combustion efficiency in the combustor and increase in the ECU reset rate.

The Model-Based Fault Detection (MBFD) technique will not only indicate which component is malfunctioning but indicate which fault is occurring and estimate the magnitude of the fault (Litt, et al., 1995). It can be used both during the pre-flight HIT check and, if desired, during flight to indicate potential faults which should be investigated before there is an actual failure.

This report has four parts: diagnostic model development, simulation of faults, results, and conclusions.

2. DIAGNOSTIC MODEL DEVELOPMENT

The objective of this part of the study was to develop experimental, open-loop, state space, diagnostic models of the T700 turboshaft engine for use in the FDD system design. Figure 1 shows a schematic diagram of the T700 turboshaft engine. An open-loop model of the T700 engine has been developed consisting of the HMU, gas generator, and power turbine as a unit.
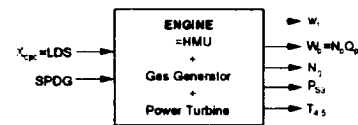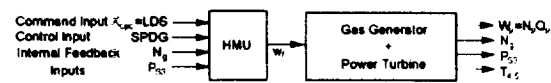
The description of the operation of the engine and the engine variables can be found in Duyar, et al. (1995), which derived an experimental, open-loop model of the T700 gas generator and power turbine as a unit. The actuation mechanism, i.e., the HMU and associated fuel system components[1] were not, however, included. Duyar, et al. (1995) used input fuel flow variations to develop the experimental model of the gas generator and the power turbine. In the work reported here, on the other hand, the collective and ECU command signals were used as input to the HMU, thus restricting fuel flow variations to those which the HMU could physically produce. This yields an improvement in the gas generator and power turbine model, since the model parameters are fit to a more realistic set of input variations.

Prior to actually generating the experimental state space models, open-loop block diagrams were developed such that the engine is separated from the rotor system. This approach makes it possible for the open-loop models to be used, not only for fault detection and diagnosis system design, but also for control design purposes and for simulation studies to determine the effect of using different rotor systems. The block diagrams were developed by considering the physical processes occurring in the components, the constraints imposed by the available tool for generation of the experimental data, i.e., the simulation developed by Ballin (1988), and the variables that are affected by faults. The simplified open-loop block diagrams developed are shown in figure 2. The closed-loop diagram is presented in figure 3. The first step in the development of these block diagrams was to construct a major functions/components diagram using the information in Litt, et al. (1995), Ballin (1988), and Prescott and Morris (1987).

---

[1]   In this work the various parts of the fuel regulating system associated with the HMU (Fuel Boost Pump, Pressurizing and Overspeed Unit (POU), and Fuel Injectors) are referred to collectively as the HMU.

2

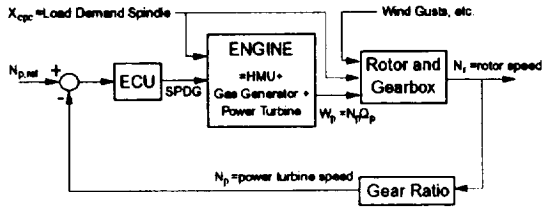$$x(n+1) = A \ x(n) + B \ u(n) \qquad (1)$$

$$y(n) = C \ x(n) \qquad (2)$$

Figure 3. T700 Closed-Loop Block Diagram
(ECU and HMU are represented by simplified models)

Emphasis was placed on identification of the fuel control-related components which are replaced during AVUM and AVIM level trouble-shooting procedures. The block diagrams shown in figure 2 and figure 3 were obtained by simplifying this major functions/components diagram, while ensuring that the significant functionalities were maintained.

Careful evaluation of the physical processes in turbine engines shows that, for a stand-alone model of the engine (one which can be used with different rotor systems), the essential output of the engine is power, W_P. Under ideal conditions, the power is a function of only the conditions produced by the gas generator at the power turbine entrance. Power turbine power is fed to the load—the rotor system of the specific aircraft. This power is the product of the power turbine torque, Q_P, and the power turbine speed, N_P, which are both measured quantities. The load dynamics determine the split of the power between speed and torque at any particular time.

Additional outputs of the engine which show the effects of the faults are the fuel flow rate, w_f, the gas generator speed, N_g, power turbine inlet temperature, T_{45}, and the compressor final stage pressure, P_{S3}. The inputs to the HMU/engine system are the collective pitch angle, X_{cpc}, and the trim signal from the electrical control unit, SPDG. The power available spindle angle, PAS, and the inlet air temperature, T_2, are assumed to be constant in this study and therefore are not included as inputs. Under normal operation of the engine PAS is regularly kept at a constant angle. Therefore the model developed in this study is restricted to normal flight conditions or testing at these conditions.

It is assumed that the nonlinear open-loop dynamics of the engine can be normalized and linearized about a nominal operating condition and can be expressed as a discrete-time linear system described by the following state equations

where x, u, and y are the m×1 state, the p×1 input, and the q×1 output vectors, respectively. A, B, C are the known nominal matrices of the system with appropriate dimensions. The process noise, measurement noise, and the modeling errors due to uncertainties in the parameters are not included for mathematical simplicity. It is assumed that the system is in α-canonical form (Litt, et al., 1995).

The procedure explained in Duyar, et al. (1995) was followed to obtain the experimental model. A three-level pseudo random sequence was used for the ECU trim signal input. A modified version of this three level signal, where changes from one level to another occur through a ramp function rather than a step function, was used for the collective input. This modification is warranted because the collective input is a mechanical input and cannot change instantaneously. Figure 4 shows these input signals used to identify the open-loop engine model.

Most of the interaction between the rotor, drive train, and engine takes place at or below the main rotor frequency of about 300 rpm. Thus it is important that the simulation be accurate in the range below 5 Hz. Therefore a clock time of 2 seconds and a length of 26 was used with the three level sequences. Sampling time was selected to be 0.1 second. This corresponds to a maximum frequency of 31.4 rad/sec (5 Hz), a minimum frequency of 0.24 rad/sec (0.04 Hz), and a signal duration of 26 sec.

For the purposes of this study the A, B, and C matrices were obtained for the single power level of approximately 100%. Table 1 presents the resultant open-loop state space engine model.

3. SIMULATION OF FAULTS

It is important to understand which components realistically may fail and how these failures may be reflected in observable engine outputs in order to construct a meaningful diagnostic model. To this end the Aviation Unit and Intermediate Maintenance Manual (T700, 1981) for the T700 helicopter engine was reviewed to identify faults dealt with at the AVUM and AVIM levels. The trouble-shooting procedures in the manual were studied together with information on the components involved found in Prescott and Morris (1987) and Ballin (1988) to identify potential faults to be considered. These faults are presented in Table 2.

3

x	A					B		u
N_g^*	1.1522	0.0042	0.0975	-0.1043	-0.0028	-0.0034	0.0066	SPDG*
W_p^*	1.7486	0.9596	0.6840	-0.7971	-0.1771	-0.0559	0.1228	X_{cpc}^*
T_{45}^*	0.7718	0.4339	1.0821	-0.8655	-0.3867	-0.0994	0.1433	
P_{S3}^*	1.1269	-0.0271	0.4144	0.4985	-0.0177	-0.0137	0.0325	
w_f^*	2.9536	1.1513	0.4429	-2.6096	-0.0402	-0.2603	0.3738	

y	C					The asterisk, *, indicates that the elements of the **u**, **x**, and **y** vectors are normalized perturbations from the initial, steady-state values of the indicated parameters: $$z^* = (z - z_0)/\, z_0.$$
N_g^*	1.0	0.0	0.0	0.0	0.0	
W_p^*	0.0	1.0	0.0	0.0	0.0	
T_{45}^*	0.0	0.0	1.0	0.0	0.0	
P_{S3}^*	0.0	0.0	0.0	1.0	0.0	
w_f^*	0.0	0.0	0.0	0.0	1.0	

Table 1. Open-Loop State Space Engine Model at 100% N_g

Two of the potential actuator faults listed in Table 2 were selected to illustrate the method. One was chosen to be essentially at an "entrance" to the HMU. The other is essentially at the "exit." For the entrance, increasing friction in the torque motor is emulated by an increasing value of the torque motor lag. (The appendix details the basis for modeling this fault.) For the exit, a clogging fuel metering valve is emulated by multiplying the flow through the valve by a factor less than one.

Two additional faults, which are outside the actuation system, have also been modeled: degradation of combustion efficiency in the combustor and increase in the ECU reset rate.

4. RESULTS

Several measures for detection of faults were explored. These included using the instantaneous difference in peak values between faulted and nominal outputs, and the integral of the difference between faulted and nominal outputs. Likewise a number of different input signals were explored—periodic signals such as that for X_{cpc} in Figure 4, and as in Duyar, et al., (1995) and Ballin (1988), limited ramps and steps. (For the closed loop engine—which is what would be actually tested—the only input available is X_{cpc}. The values of SPDG used for input to the state space model were calculated by Ballin's model using the given input sequence for X_{cpc}.)

The step or ramp input in X_{cpc}, coupled with the integral of the difference between faulted and nominal output, gave satisfactory results. The other fault detection measures failed to sufficiently distinguish between faulted and nominal conditions. Since a true step input is physically impossible, a limited ramp input is recommended. The recommended input uses an increase in X_{cpc} in a five-second ramp from the initial, steady-state value to the same maximum value that is used for establishing the model (figure 4), then remains constant at that value.
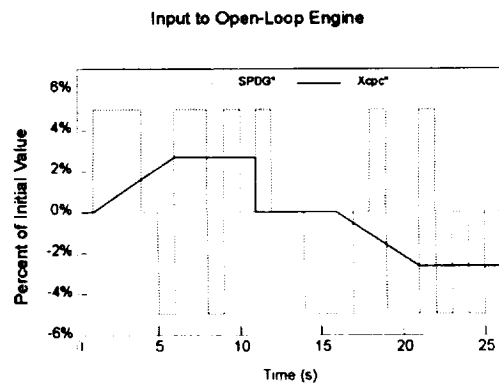
Input to Open-Loop Engine

Figure 4. Input signals used to identify open-loop engine model

4

TABLE 2. POTENTIAL FAULTS

Component	Sub-Component	Fault
Actuators		
"HMU" (For the purposes of this study the scope of the HMU has been extended beyond that of the physical component to create a functional HMU which includes the physical HMU, the fuel injectors, POU, and fuel boost pump. These components all work together to control fuel flow.)	torque motor	increased rotational friction
		decreased maximum travel
		increased deadband
	metering valve	clogging
		increased wear
		increased friction
	vane pump	increased tip leakage
		sticking vanes
	N_g spool	increased hysteresis
		increased friction
	Fuel injectors	clogging
	POU	sticking valves
	Fuel boost pump	clogging
		leaking
Sensors		
P_{S3} Hose and Tube Assembly + P_{S3} Sensor		leaking or loose hose
		faulty sensor
Power Turbine Speed Sensor		faulty sensor
Power Turbine Torque Sensor		faulty sensor
Thermocouple Assembly		faulty sensor
Yellow Electrical Cable		broken wires
		loose or corroded connections

Figure 5 shows the integrated differences between the fuel flow predicted by the state space model and those calculated by Ballin's model for a five-second ramp beginning one second into the run. Included are curves for the no-fault condition and for faults in the HMU, ECU, and combustor:

- 100% increase in the reset rate for the ECU PI controller
- 10% decrease in efficiency in the combustor
- 10% increase in HMU metering valve clogging
- 20% increase in HMU metering valve clogging

As can be seen, the slopes for increases in metering valve clogging are steeper than the no fault slope. This effect increases with increases in percent clogging. This method, therefore, yields an effective means of detecting a fault.

The difficulty lies in effectively isolating the source of the fault. Figure 5 shows a negative slope for the case where combustion efficiency has degraded, while a clogged metering valve produces a positive slope. This provides an encouraging indication that this approach can be used to help in the isolation of HMU and combustor faults. However, applying this technique

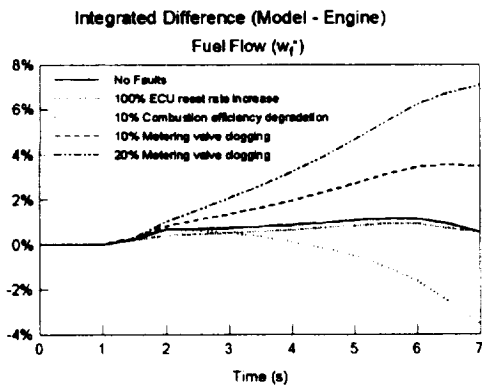Integrated Difference (Model - Engine)
Fuel Flow (w_f')

Figure 5. Integrated fuel flow difference

when the fault involved an increase in the ECU reset rate yielded a slope similar to that of the no fault case. Thus, although this method may be able to distinguish the HMU fault (metering valve clogging) from a combustor fault, without additional information it does not distinguish a faulty ECU.

5. CONCLUSIONS

A method for detection of faults originating in the actuation system of a T700 turboshaft engine has been developed and demonstrated. One can design input signals to enhance the effect of the fault. Injection of faults resulted in clearly detectable differences between actual system outputs and those calculated by the nominal model for realistic test input. A complete set of criteria can be generated to assist in isolating malfunctioning components during pre-flight engine maintenance by coupling the approach laid out here with that of Litt, *et al.* (1995) for sensor faults. Diagnostic equipment which uses this method would help focus maintenance procedures on the faulty component. This could greatly shorten the present trial and error methods for malfunction elimination.

At least three areas need to be pursued further: 1) The ECU fault could not be detected using the methods demonstrated. An ECU model might need to be incorporated into the diagnostic model in order to accomplish this. 2) The open-loop state space engine and HMU models need to be obtained for other power levels (in addition to that of 100% presented in Table 1, flight idle for instance). Together with this, techniques for joining the linear state space models at the various discrete power levels to obtain an effectively non-linear model need to be explored. 3) The approach laid out here should be integrated with that of Litt, *et al.* (1995) for sensor faults to generate a complete set of criteria to assist in isolating malfunctioning components.

6. APPENDIX: Modeling Torque Motor Faults

The torque motor is modeled in Ballin (1988) by a simple integrator, fed by filtered and limited signals. This is consistent with the discussion of servomotors on pp. 96 ff. of Ogata (1970). Ogata shows that both two-phase AC and armature-controlled DC servomotors are approximately integrators, i.e. they reduce to the form K_m/s. (Another type, field-controlled DC servomotors, has a much more complex transfer function.) For the AC motor:

$$K_m = K_c / (f + K_n)$$

where

K_c, K_n are parameters which describe the torque versus motor speed and control voltage curves, and

f   is the viscous friction coefficient of the motor and load referred to the motor shaft, i.e. the product of f and the angular speed of the motor shaft is the total torque due to friction in the motor and load.

For the field-controlled DC motor:

$$K_m = K / (R_a f + KK_b)$$
$$= (K/R_a)/[f + (KK_b/R_a)]$$

where

K   is the slope of the torque versus armature current line,

R_a is the armature winding resistance,

f   is the viscous friction coefficient of the motor and load referred to the motor shaft, i.e. the product of f and the angular speed of the motor shaft is the total torque due to friction in the motor and load, and

K_b is a back emf constant—the slope of the voltage induced in the armature by rotation versus the angular velocity.

Thus both servomotor types have transfer functions of the form K_m/s with $K_m = K_1 / (f + K_2)$, where f is the viscous friction coefficient and K_1 and K_2 relate to motor electrical characteristics. In Ballin's program, K_m is the factor TMGN, which has the value 0.0159 in/ma sec.

Let us assume that mechanical degradation is more likely than electrical degradation and that this takes the form of an increase in f:

$$f = f_0 (1 + d/100)$$

where f_0 is the nominal value of f (corresponding to TMGN = 0.0159) and d is the percent increase in f.

6

Then

$$\begin{aligned} \text{TMGN} &= K_1 / [f_0 (1 + d/100) + K_2] \\ &= \text{TMGN}_0 (f_0 + K_2) / [f_0 (1 + d/100) + K_2] \\ &= \text{TMGN}_0 \\ &\quad \times (1 + K_2/f_0) / [(1 + d/100) + K_2 / f_0] \end{aligned}$$

For $K_2/f_0 \ll 1$:

$$\text{TMGN} \approx \text{TMGN}_0 / (1 + d/100)$$

($K_2/f_0 \approx 0.03$ in the example Ogata gives in the text. In the problems at the end of the chapter, however, he presents some range of examples including one with $K_2/f_0 \approx 2.4$. Viscous friction may or may not, therefore, be a dominant effect in the torque motor. This analysis assumes it is. More detail about the specifics of the design would be necessary in order to be sure this is a valid assumption. It can also be noted that the approach taken here could be used to emulate a degradation in the electrical characteristics of the motor. The interpretation of d would change from percent increase in viscous friction factor to percent change in some electrical characteristic; but the results would remain the same.)

This is implemented in Ballin's program by using

$$\text{TMGN} \approx \text{TMGN}_0 / \text{tqMotFricFac}$$

i.e. tqMotFricFac = (1 + d/100). It is assumed that d is never negative and, therefore, tqMotFricFac is limited to be greater than or equal to one.

Figure A-1 shows the variation in Standard Error Estimate (SEE) with d, the percent increase in friction factor. These results are for the open loop engine (figure 2) using the inputs shown in figure 4. SEE is the square root of the value obtained by dividing the sum of the squares of the difference between the state space result (which does not include any effect of a change in d) and the output of Ballin's model (with the changed d) by the sum of the squares of the output of Ballin's model. RMS is the root mean squared average of the five outputs.

Standard Error Estimates (SEEs)
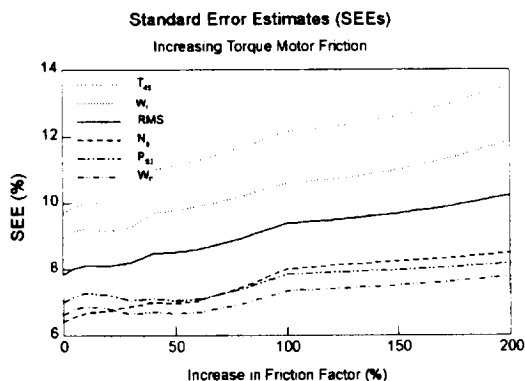
Increasing Torque Motor Friction

Figure A-1 Effect of Increase in Torque Motor Friction

It is clear that under ideal conditions, changes in d greater than about 25% are observable. It is likely, however, that under normal operating conditions, changes in d would need to be at least of the order of 100% before they are noticed, i.e., the viscous friction would probably have to double, or more, to produce a distinct difference in the SEEs. On the other hand, if changes in d of less than 100% produce little observable change in the SEEs, they may also produce little effect on engine performance. It may be that an HMU is not faulty (with respect to the torque motor) unless the viscous friction more than doubles.

8. REFERENCES
Aerospace Engineering (1995). "Artificial Intelligence for Turbine Engine Diagnostics," *Aerospace Engineering*, March 1995, pp. 9-13.

Ballin, M. G. (1988). "A High Fidelity Real-Time Simulation of a Small Turboshaft Engine," NASA Technical Memorandum 100991.

Duyar, A., V. Eldem, W. Merrill, and T.-H. Guo (1994). "Fault Detection and Diagnosis in Propulsion Systems: A Fault Parameter Estimation Approach," *AIAA Journal of Guidance, Control and Dynamics*, 17, No. 1, pp. 104-108.

Duyar, A., Z. Gu and J. Litt (1995). "A Simplified Dynamic Model of the T700 Turboshaft Engine," *Journal of the American Helicopter Society*, 40, No. 4, pp. 62-70.

Litt, J., M. Kurtkaya and A. Duyar (1995). "Sensor Fault Detection and Diagnosis of the T700 Turboshaft Engine," *AIAA Journal of Guidance, Control and Dynamics*, 18, No. 3, pp. 640-642.

Ogata, K. (1970). *Modern Control Engineering*, Prentice-Hall, Inc., Englewood Cliffs, NJ.

Prescott, W. E. and H. F. Morris (1987). *T700 Training Guide*, General Electric Company, Lynn, MA.

T700 (1981). *Aviation Unit and Intermediate Maintenance Manual: Engine, Aircraft: Turboshaft: Models T700-GE-700, T700-GE-701, T700-GE-701C*, Army TM 55-2840-248-23, Air Force T.O. 2J-T700-6.

REPORT DOCUMENTATION PAGE

Public reporting burden for this collection of information is estimated to average 1 hour per response, including the time for reviewing instructions, searching existing data sources, gathering and maintaining the data needed, and completing and reviewing the collection of information. Send comments regarding this burden estimate or any other aspect of this collection of information, including suggestions for reducing this burden, to Washington Headquarters Services, Directorate for Information Operations and Reports, 1215 Jefferson Davis Highway, Suite 1204, Arlington, VA 22202-4302, and to the Office of Management and Budget, Paperwork Reduction Project (0704-0188), Washington, DC 20503.

1. AGENCY USE ONLY (Leave blank)	2. REPORT DATE	3. REPORT TYPE AND DATES COVERED
	November 1998	Technical Memorandum

4. TITLE AND SUBTITLE	5. FUNDING NUMBERS
Model–Based Fault Diagnosis for Turboshaft Engines	WU–505–62–50–00
6. AUTHOR(S)	1L161102AH45
Michael D. Green, Ahmet Duyar, and Jonathan S. Litt	

7. PERFORMING ORGANIZATION NAME(S) AND ADDRESS(ES)	8. PERFORMING ORGANIZATION REPORT NUMBER
NASA Lewis Research Center Cleveland, Ohio 44135–3191 and U.S. Army Research Laboratory Cleveland, Ohio 44135–3191	E–11433

9. SPONSORING/MONITORING AGENCY NAME(S) AND ADDRESS(ES)	10. SPONSORING/MONITORING AGENCY REPORT NUMBER
National Aeronautics and Space Administration Washington, DC 20546–0001 and U.S. Army Research Laboratory Adelphi, Maryland 20783–1145	NASA TM—1998-208825 ARL–TR–1447

11. SUPPLEMENTARY NOTES

12a. DISTRIBUTION/AVAILABILITY STATEMENT	12b. DISTRIBUTION CODE
Unclassified - Unlimited Subject Category: 07 Distribution: Nonstandard This publication is available from the NASA Center for AeroSpace Information, (301) 621–0390.	

13. ABSTRACT (Maximum 200 words)

Tests are described which, when used to augment the existing periodic maintenance and pre–flight checks of T700 engines, can greatly improve the chances of uncovering a problem compared to the current practice. These test signals can be used to expose and differentiate between faults in various components by comparing the responses of particular engine variables to the expected. The responses can be processed on–line in a variety of ways which have been shown to reveal and identify faults. The combination of specific test signals and on–line processing methods provides an *ad hoc* approach to the isolation of faults which might not otherwise be detected during pre–flight checkout.

14. SUBJECT TERMS			15. NUMBER OF PAGES
Turboshaft engines; Diagnostics; Fault detection			13
			16. PRICE CODE
			A03

17. SECURITY CLASSIFICATION OF REPORT	18. SECURITY CLASSIFICATION OF THIS PAGE	19. SECURITY CLASSIFICATION OF ABSTRACT	20. LIMITATION OF ABSTRACT
Unclassified	Unclassified	Unclassified	